Molecular Pharmacology Fast Forward. Published on August 28, 2012 as doi:10.1124/mol.112.080275

Identification of Structural Motifs Critical for EBI2 Function and Homology Modeling of Ligand Docking Site

Li Zhang, Amy Y. Shih, Xia V. Yang, Chester Kuei, Jiejun Wu, Xiaohu Deng, Neelakandha S. Mani, Taraneh Mirzadegan, Siquan Sun, Timothy W. Lovenberg, Changlu Liu

Janssen Pharmaceutical Research and Development, L.L.C., 3210 Merryfield Row, San Diego, California (L.Z., A.Y.S., X.V.Y., C.K., J.W., X.D., N.S.M., T.M., S.S., T.W.L., C.L.)

Molecular Pharmacology Fast Forward. Published on August 28, 2012 as DOI: 10.1124/mol.112.080275
This article has not been copyedited and formatted. The final version may differ from this version.

Running title: An insight into the structural basis of EBI2 function

Address correspondence to:

Changlu Liu

Janssen Pharmaceutical Research and Development, LLC

3210 Merryfield Row

San Diego, California 92121

Tel: 858-784-3059

Fax: 858-784-3085

E-mail: CLiu9@its.jnj.com

Total text pages: 38

Tables: 2

Figures: 4

References: 24

Number of words in the Abstract: 246

Number of words in the Introduction: 749

Number of words in the Discussion: 1498

Abbreviations: β2AR, β2-adrenergic receptor; EBI2, Epstein-Barr virus-induced molecule-2; ECL, extracellular loop; ELISA, enzyme-linked immunosorbent assay; GPCR, G protein-coupled receptor; GTPγS, guanosine5'-*O*-(3-thio)triphosphate; OHC, hydroxycholesterol; TM, transmembrane.

Molecular Pharmacology Fast Forward. Published on August 28, 2012 as DOI: 10.1124/mol.112.080275
This article has not been copyedited and formatted. The final version may differ from this version.

Abstract

Epstein-Barr virus-induced molecule-2 (EBI2, also known as GPR183) is a G-protein-coupled receptor (GPCR) best known for its role in B cell migration and localization. Our recent deorphanization effort led to the discovery of 7α,25-dihydroxycholesterol (7α,25-OHC) as the endogenous ligand for EBI2, providing a tool for the mechanistic studies of EBI2's function. Since EBI2 is the first GPCR known to bind and be activated by an oxysterol, the goal of this study was to understand the molecular and structural basis for its ligand-dependent activation. This was achieved by identifying structural moieties in EBI2 or in 7α,25-OHC that may impact the receptor-ligand interaction. Using a series of chemically related OHC analogs, we demonstrated that all three hydroxyl groups in 7α,25-OHC contribute to ligand-induced activation of the receptor. To elucidate the location and composition of the ligand-binding domain in EBI2, we used a site-directed mutagenesis approach and generated mutant receptors that carry single amino acid substitution at selected residues of interest. Biochemical and pharmacological profiling of these mutant receptors allowed for structure-function analysis and revealed critical motifs that likely interact with 7α,25-OHC. Using a hybrid β2AR-CXCR4 structure as template, we created a homology model for EBI2 and optimized the docking of 7α,25-OHC into the putative ligand binding site so that the hydroxyl groups interact with residues Arg87, Asn114, and Glu183 respectively. This model of ligand-docking brings important structural insight into the molecular mechanisms mediating EBI2 function, and may facilitate future efforts to design novel therapeutic agents that target EBI2.

Molecular Pharmacology Fast Forward. Published on August 28, 2012 as DOI: 10.1124/mol.112.080275
This article has not been copyedited and formatted. The final version may differ from this version.

Introduction

Epstein-Barr virus-induced molecule-2 (EBI2), also known as GPR183, is a GPCR originally identified as a gene highly up-regulated upon Epstein-Barr virus (EBV) infection (Birkenbach et al., 1993). EBI2 is expressed most abundantly in lymphoid tissues, such as spleen and lymph nodes (Birkenbach et al., 1993; Rosenkilde et al., 2006). Although classified as a Class A rhodopsin-like GPCR (Vassilatis et al., 2003), EBI2 lacks high sequence similarity to most other GPCRs. The closest homolog is GPR18 which shares 52% similarity to EBI2 (Benned-Jensen and Rosenkilde 2008). Previous studies have shown EBI2 signals through $G_{\alpha i}$, but not $G_{\alpha s}$ or $G_{\alpha q}$ (Rosenkilde et al., 2006; Liu et al., 2011; Hannedouche et. al., 2011). Activation of EBI2 leads to adenylate cyclase inhibition and subsequent reduction of cAMP production. EBI2 has also been reported to activate extracellular signal-regulated kinase (Benned-Jensen et al., 2011).

Significant progress has been made recently that has helped to unveil the functional significance of EBI2 in the immune system (Pereira et al., 2009; Gatto et al., 2009; Liu et al., 2011; Hannedouche et al., 2011; Kelly et al., 2011; Gatto et al., 2011). It is now widely acknowledged that EBI2 and EBI2-mediated chemotaxis represent an important molecular mechanism for directing follicular B cell migration and localization. Up-regulation of EBI2 in B cells during early stages of an immune response promotes the movement of activated B cells to the outer- and inter-follicular regions, while down-regulation of EBI2 allows B cell to move to the center of follicles for germinal center formation. These carefully orchestrated events are part of an intricate and well-balanced

Molecular Pharmacology Fast Forward. Published on August 28, 2012 as DOI: 10.1124/mol.112.080275
This article has not been copyedited and formatted. The final version may differ from this version.

network of chemokine receptors that includes EBI2, CXCR5, CCR7 and CXCR4 (Gatto et al., 2011; Kelly et al., 2011). Together, they are responsible for providing B cells with a precise roadmap for mounting a correct antibody response when it is needed. B cells from EBI2-deficient mice have been reported to have an abnormal migration pattern and reduced antibody response (Liu et al., 2011).

Recently we identified an oxysterol, 7α,25-OHC, as the most likely endogenous ligand for EBI2 (Liu et al., 2011). 7α,25-OHC (structure shown in Fig. 2A) is an oxygenated derivative of cholesterol and is converted endogenously from 25-hydroxycholesterol (25-OHC) by the enzyme CYP7B1 (Rose et al., 1997). 7α,25-OHC binds EBI2 with a dissociation constant of 450 pM and activates EBI2 with an EC_{50} of 140 pM, more potent than any of the other oxysterols we have tested. Functionally, 7α,25-OHC directs B cell migration both *in vitro* and *in vivo*. Pharmacological blockade of 7α,25-OHC synthesis disrupts B cell migration patterns, consistent with what has been observed with B cells from EBI2-deficient mice (Liu et al., 2011). Similar results were reported by Hannedouche and colleagues (Hannedouche et al., 2011).

Identification of 7α,25-OHC as the endogenous ligand for EBI2 has revealed an important link between EBI2 and its known function in the immune system and allowed us to measure receptor activation quantitatively *in vitro.* Previous structure-function studies of EBI2 were largely focused on investigating its constitutive activity. These studies revealed important structural motifs for the ligand-independent activity of this

Molecular Pharmacology Fast Forward. Published on August 28, 2012 as DOI: 10.1124/mol.112.080275
This article has not been copyedited and formatted. The final version may differ from this version.

receptor and suggested potential molecular constraints during receptor transition from the inactive to the active conformation (Benned-Jensen and Rosenkilde, 2008; Benned-Jensen et al., 2011). We decided to explore the molecular mechanisms of ligand-dependent activation of EBI2 using 7α,25-OHC as a tool. We have previously shown that the hydroxyl groups in the 7' and 25' positions of 7α,25-OHC are important for ligand activity (Liu et al., 2011). Here we further demonstrated that the 3'-hydroxyl group, native to the cholesterol steroidal body, is also a critical component of the receptor–ligand interaction. To dissect out the structural motifs in EBI2 that are important for receptor activity, we used a mutagenesis approach and made single amino acid changes at various positions of the receptor, the majority of which are side-chain eliminations with Ala substitutions. Transmembrane region mutations were proposed based on sequence alignment of EBI2 to GPCRs with known x-ray crystal structures. Mutations in the extracellular loops were mainly proposed based on conservation among different species (Fig. 1). By measuring receptor expression, receptor activation, and radioligand binding, we characterized the pharmacological profiles of mutant receptors and identified key residues mediating receptor function. These structure-activity data were incorporated into a homology model of EBI2. Using a hybrid β2AR-CXCR4 structure as template, we were able to dock 7α,25-OHC and define the putative ligand binding site. We believe this information will facilitate the rational design of small molecule compounds that may serve as agonists or antagonists for EBI2.

Molecular Pharmacology Fast Forward. Published on August 28, 2012 as DOI: 10.1124/mol.112.080275
This article has not been copyedited and formatted. The final version may differ from this version.

Materials and Methods

Materials

All materials, except where indicated, were purchased from Sigma-Aldrich (St. Louis, MO). 7α,25-OHC, 7α,27-OHC, and 7α,27-dihydroxy-4-cholesten-3-one were purchased from Avanti Polar Lipids (Alabaster, AL). ^{3}H-labelled 7α,25-OHC was custom synthesized by Moravek Biochemicals (Brea, CA) (specific activity: 30 Ci mmol^{-1}). Cell culture reagents were purchased from Hyclone (Logan, UT). Lipofectamine transfection reagent and anti-V5 mouse monoclonal antibody were purchased from Life Technologies (Carlsbad, CA).

Site-Directed Mutagenesis for EBI2

The coding region of human ebi2 (GenBank accession number NM_004951.4) with a V5-tag at the N-terminus (V5-ebi2) was cloned into the mammalian expression vector pCIneo as described (Liu et al., 2011). For site-directed mutagenesis, wildtype V5-ebi2 served as template for PCR-amplifications using primers that contained the mutated sequence. The mutated ebi2 DNA was inserted back into pCIneo vector and all constructs were verified by DNA sequencing at Eton Biosciences (San Diego, CA). For a complete list of the mutations, see supplemental Table 1.

Tissue Culture and Recombinant Expression of mutant human EBI2

COS7 cells were grown in Dulbecco's Modified Eagle Medium (with 4500 mg/L glucose, 10% fetal bovine serum, 1% penicillin–streptomycin, 1 mM sodium pyruvate, 20 mM

Molecular Pharmacology Fast Forward. Published on August 28, 2012 as DOI: 10.1124/mol.112.080275
This article has not been copyedited and formatted. The final version may differ from this version.

HEPES) at 5% CO_2 and 37^{o}C. Transient transfections of COS7 cells were performed using Lipofectamine reagent in Opti-MEM media according to manufacturer's manual. For receptor expression characterization, cells were transiently transfected with V5-tagged ebi2 alone. For GTPγS and radioligand binding assays, cells were co-transfected with ebi2 constructs plus a human G protein, G_{O2}, expression construct which contains the coding region of the human G_{O2} (GenBank Accession No. AF493895) in the mammalian expression vector pcDNA3.1/zeo. The transfected cells were harvested 48 hrs later and cell pellets were stored at −80 °C until GTPγS and radioligand binding assays could be performed.

Characterization of Receptor Expression

To assess total and cell-surface receptor expression levels, transiently transfected cells were seeded in 96-well culture plates in triplicates (4 x 10^4 cells/well) 24 hrs after transfection. Cells were then fixed with 4% paraformaldehyde two days post transfection. Total and cell-surface expressions of V5-tagged receptor proteins were quantified by ELISA using Anti-V5 antibody (1 µg/ml) either in the presence of 1% Triton-X-100 (for total protein detection) or in the absence of Triton-X-100 (for cell-surface protein expression). Cells transfected with G_{O2} expression construct alone were used as negative controls. Cells transfected with wildtype V5-ebi2 construct were used as positive control. Cells transfected with GPR81-V5, a GPR81 expression construct with a V5-tag at the C-terminus were also included as controls.

Molecular Pharmacology Fast Forward. Published on August 28, 2012 as DOI: 10.1124/mol.112.080275
This article has not been copyedited and formatted. The final version may differ from this version.

GTPγS Binding Assay

^{35}S-GTPγS binding assay was performed as described (Liu et al., 2003). Briefly, membrane preparations from transfected cells were added to 96-well plates and incubated with different concentrations of ligand at room temperature for 20 min. ^{35}S-GTPγS (PerkinElmer Life Sciences, Waltham, MA) was then added to the mixture at a final concentration of 200 pM. The reactions were allowed to proceed at room temperature for 1 hr, filtered though a 96-well GFC filter plate (Packard Instrument Company, Meriden, CT) and washed with buffer (20 mM Tris-HCl, 10 mM $MgCl_2$, pH 7.4). 50 µL of Microscint-40 (PerkinElmer Life Sciences) was added to each well and the plate was counted on a Top Counter (TopCount NXT, Packard, Meriden, CT). Assays were performed in triplicate and analyzed with GraphPad Prism 5 software (GraphPad, San Diego, CA). ^{35}S-GTPγS incorporation in the presence of ligand activation was normalized as a percentage increase over basal counts in the absence of ligands. EC_{50} values were calculated as the ligand concentration that stimulated 50% of the maximum response (E_{max}). For comparison among different mutant receptors, the maximum response of the wildtype EBI2 to 7α,25-OHC was expressed as 100% and used to compare the maximum GTPγS incorporation for all other mutant receptors. The EC_{50} and E_{max} values for mutants that did not reach a plateau in the GTPγS binding assay at the highest concentration of ligand used (1 µM for 7α,25-OHC, 10 µM for 7α,27-dihydroxy-4-cholesten-3-one) were not calculated.

Molecular Pharmacology Fast Forward. Published on August 28, 2012 as DOI: 10.1124/mol.112.080275
This article has not been copyedited and formatted. The final version may differ from this version.

Radioligand Binding Assay

[^{3}H]7α,25-OHC was used in competition binding experiments as described previously (Liu et al., 2001; Liu et al., 2011). Briefly, membrane preparations from COS7 cells that transiently express wildtype or mutant EBI2 were incubated with [^{3}H]7α,25-OHC (100,000 c.p.m.) in the presence of a series of concentrations of unlabelled 7α,25-OHC as a competitor. We used unlabelled 7α,25-OHC as the competitor because it has the highest affinity to EBI2 and best solubility. We previously showed that using mock transfected COS7 cells, unlabeled 7α,25-OHC (1 μM) did not displace significant binding in mock transfected COS7 cells (Liu et al., 2011). Other available ligands have lower affinities for EBI2 and/or are much more hydrophobic. To use those ligands at concentrations saturating EBI2 binding often lead to solubility issues. The reactions were incubated at room temperature for 1 hr and then filtered though the 96-well GFC filter plate and washed with buffer (20 mM Tris-HCl, 10 mM $MgCl_2$, pH 7.4) three times. The bound radioligand was counted on the Top Counter and the results were analyzed using GraphPad Prism 5 software. The maximum specific binding of the wildtype EBI2 to [^{3}H]7α,25-OHC was expressed as 100% and used to compare the radioligand binding of mutant receptors.

Molecular Modeling

Homology modeling of human EBI2 and subsequent docking of 7α,25-OHC was done using Discovery Studio 3.1 (Accelrys, San Diego, CA). The primary sequence alignment between human β2-adrenergic receptor (β2AR) and EBI2 was determined using the

Molecular Pharmacology Fast Forward. Published on August 28, 2012 as DOI: 10.1124/mol.112.080275
This article has not been copyedited and formatted. The final version may differ from this version.

align123 program implemented in Discovery Studio. The helical alignment was further examined and manually refined based on a multiple sequence alignment of family A GPCRs (Mirzadegan et al., 2003). The β2AR structure (PDB code 2RH1) was used as a template for EBI2 except for TM2 and ECL2 which used CXCR4 (PDB code 3ODU) as a template. Each of the CXCR4 components was separately aligned to the β2AR structure to produce a hybrid β2AR-CXCR4 template structure. Based on this hybrid template structure, an EBI2 homology model was built using the homology modeling component of Discovery Studio.

The EBI2 homology model was placed into a 30 Å thick implicit membrane and energy minimized using the Smart Minimizer algorithm with Generalized Born with Implicit Membrane implicit solvent model using the CHARMm forcefield. 7α,25-OHC was manually docked into the ligand binding site of the model EBI2 structure based on GTPγS binding and radioligand binding assay data (Table 2). Once the ligand was docked into the binding site, a standard dynamics cascade (which includes steepest decent minimization, conjugate gradient minimization, heating of the system to 300K, molecular dynamics equilibration, and production runs) was performed with the ligand constrained. The constraints on the ligand were then removed and the entire system was further minimized to generate the final model of EBI2 with 7α,25-OHC docked.

Molecular Pharmacology Fast Forward. Published on August 28, 2012 as DOI: 10.1124/mol.112.080275
This article has not been copyedited and formatted. The final version may differ from this version.

Results

Effect of Ligand Structure on EBI2 Activation.

^{35}S-GTPγS binding assay was used for quantifying receptor activation. This assay measures the binding of a non-hydrolysable ^{35}S-GTPγS to the G_{α} subunit following agonist occupation of the receptor and has the advantage of measuring one of the earliest receptor-mediated events in the signaling cascade and is less affected by downstream signaling amplification or modulation. We transfected COS7 cells with EBI2 expression constructs in combination with G_{O2} protein because our previous studies have shown that co-expression of G_{O2} increases the ligand-stimulated ^{35}S-GTPγS incorporation and improves signal/noise ratio (Liu et al., 2011).

Previously we showed that 7α,25-OHC activates EBI2 with high affinity and potency in recombinant systems (K_d = 450 pM; EC_{50} = 140 pM, Liu et al., 2011). We also screened a series of other oxysterols and cholesterol derivatives for their abilities to activate EBI2. Of the compounds that showed agonist activity, we ranked them based on ligand potency: 7α,25-OHC (EC_{50}=0.14 nM) > 7α,27-OHC (EC_{50}=1.3 nM) > 7β,25-OHC (EC_{50}=2.1 nM) > 7β,27-OHC (EC_{50}=51 nM) > 7α-OHC (EC_{50}=82 nM) > 25-OHC (EC_{50}=127 nM) > 7β-OHC (EC_{50}=1763 nM) > 27-OHC (EC_{50}=3029 nM) (Liu et al., 2011). This result strongly suggested that the hydroxyl groups in the 7' position, 25' or 27' position are important for EBI2 activation. It is important to note that cholesterol has a hydroxyl group at the 3' position of the ring structure and this hydroxyl group is present in all the oxysterols we previously tested. The importance of the 7' and 25' hydroxyl groups

Molecular Pharmacology Fast Forward. Published on August 28, 2012 as DOI: 10.1124/mol.112.080275
This article has not been copyedited and formatted. The final version may differ from this version.

for EBI2 activation prompted us to ask whether the third hydroxyl group in 7α,25-OHC at the 3' position might also play a role. To assess the functional significance of the 3'-hydroxyl group, we tested 7α,27-dihydroxy-4-cholesten-3-one which is structurally similar to 7α,27-OHC except that its 3'-position has a ketone group instead of a hydroxyl group (Fig. 2A). Consistent with our previous report, we confirmed that 7α,27-OHC showed high potency at activating EBI2 (Fig. 2B, Table 1). In contrast, 7α,27-dihydroxy-4-cholesten-3-one at concentrations up to 10 μM showed little activity in stimulating ^{35}S-GTPγS incorporation by EBI2-expressing membranes (Fig. 2B, Table 1), supporting the hypothesis that the 3' hydroxyl group is also critical for maintaining agonist activity.

Biochemical Analysis of Receptor Expression Levels for the Wildtype and Mutant EBI2.

To quantify receptor expression, we inserted a V5-tag to the N-terminal region of the wildtype and mutant EBI2. In our previous study we demonstrated that the N-terminal V5-tag does not affect EBI2 signaling (Liu et al., 2011). An anti-V5 antibody was used to label receptor proteins in transfected cells. Most mutant receptors showed similar total and cell-surface expressions as the wildtype receptor when protein levels were quantified by ELISA (supplemental Table 1). Three mutations, Cys104Ala (ECL1), Cys181Ala (ECL2) and Phe257Ala (TM6), showed about 50% reduction in total protein expression compared to wildtype EBI2 (Table 2), suggesting these three residues may be important for the biosynthesis or protein stability of EBI2. For cell-surface receptor expression, several mutations resulted in a substantial reduction, including Cys21Ala (N-

Molecular Pharmacology Fast Forward. Published on August 28, 2012 as DOI: 10.1124/mol.112.080275
This article has not been copyedited and formatted. The final version may differ from this version.

terminus), Cys104Ala (ECL1), Cys181Ala (ECL2), Cys280Ala (ECL3), Pro85Ala (TM2), Tyr90Ala (TM2), Asn114Ala (TM3), and Phe257Ala (TM6) (Table 2). These residues may be important for the proper folding, trafficking and correct insertion of receptors to the cell membrane.

Investigation of Cysteine Residues at the Extracellular Regions of EBI2.

There are four Cys residues in the extracellular regions of EBI2: Cys21 (N-terminus), Cys104 (ECL1), Cys181 (ECL2) and Cys280 (ECL3). We mutated these four Cys residues to Ala individually to see whether receptor expression, receptor function and/or ligand binding were affected. Cys104Ala and Cys181Ala mutations resulted in the complete loss of cell-surface receptor expression while maintaining similar levels of total receptor protein as the wildtype EBI2 (Table 2), suggesting Cys104 and Cys181 may be critical for the proper folding, trafficking or insertion of EBI2 to the cell membrane. No signal was detected for these two mutants in GTPγS binding assay or radioligand binding assay (Fig. 3A, Table 2). Ala substitution at Cys21 or Cys280 led to 70-80% reduction in cell-surface receptor expression and about 50% reduction in total protein expression (Table 2), indicating additional roles in receptor biogenesis. When compared to the wildtype EBI2 using GTPγS binding assay, Cys21Ala mutation in the N-terminus caused a 20-fold increase in the EC_{50} of 7α,25-OHC and about 75% decrease in E_{max} (Fig. 3A, Table 2). We didn't detect any specific binding signal for Cys21Ala mutant receptor, probably due to reduced ligand binding affinity and reduced cell-surface receptor expression. Cys280Ala mutation in ECL3 resulted in a relatively more moderate

Molecular Pharmacology Fast Forward. Published on August 28, 2012 as DOI: 10.1124/mol.112.080275
This article has not been copyedited and formatted. The final version may differ from this version.

reduction in receptor activity (EC_{50}= 0.93 nM for ^{35}S-GTPγS incorporation, Fig. 3A) and radioligand binding (16.56% of wildtype EBI2) (Table 2).

Mutations for Conserved Residues at the Extracellular Regions of EBI2.

The extracellular regions of GPCRs are highly variable but may contain important motifs for ligand binding and/or receptor activation. We compared EBI2 sequence from human, rat and mouse (Fig. 1A) and selected a number of conserved residues for mutagenesis study (Fig. 1B). For example, the ECL2 contains a highly conserved region ($T^{180}C^{181}M^{182}E^{183}Y^{184}P^{185}N^{186}F^{187}E^{188}$). We made single Ala substitution at these positions and characterized the mutant receptors pharmacologically. We also included in our study two single nucleotide polymorphisms (SNPs) in the extracellular region, M93I (ECL1) and H284Y (ECL3), as listed in the NCBI SNP database: www.ncbi.nlm.nih.gov/SNP/snp_ref.cgi?locusId=1880). Our results showed that most of these mutants had comparable levels of receptor expression and similar pharmacological profile as the wildtype EBI2 (Table 2, Supplemental Table 1). Besides Cys181 as mentioned earlier, we found that Ala substitution for Glu183 in ECL2 resulted in a great reduction in the radioligand binding signal (11.33% of wildtype), even though cell-surface expression was only moderately decreased (59.82% of wildtype, Table 2). In agreement with the radioligand binding data, Glu183Ala mutation resulted in an almost 50-fold reduction in ligand potency when tested in the GTPγS binding assay (Fig. 3B, Table 2).

Molecular Pharmacology Fast Forward. Published on August 28, 2012 as DOI: 10.1124/mol.112.080275
This article has not been copyedited and formatted. The final version may differ from this version.

Mutation Studies at the Transmembrane Regions of EBI2.

Transmembrane regions of GPCRs are structurally highly conserved and the helical cores are thought to make up the ligand binding pocket. Based on a method developed by Mirzadegan and colleagues (Mirzadegan et al., 2003), we did a sequence alignment of EBI2 to GPCRs that have known crystal structures and well-characterized ligand binding sites. Residues in EBI2 that have been aligned at the corresponding sequence positions to the known ligand binding site of GPCRs were selected for our mutation study (Fig. 1B).

As mentioned above, Pro85Ala (TM2), Tyr90Ala (TM2), Asn114Ala (TM3), and Phe257Ala (TM6) resulted in 50% or more reduction in cell-surface receptor expression. Although the Asn114Ala mutant still had 50% cell-surface expression, its maximum radioligand binding was only about 15.98% compared to the wildtype. Moreover, this mutant receptor is non-functional because no GTPγS binding could be detected even at 1 μM of 7α,25-OHC (Fig. 3D, Table 2).

We also found a series of mutations in the transmembrane regions that didn't affect cell-surface receptor expression but nevertheless had a negative impact on receptor activity in GTPγS assay (Fig. 3, Table 2). In order to understand whether the functional disruption is due to its inability to bind 7α,25-OHC, we tested these mutants in the radioligand binding assay. For comparison of ligand binding, we were only able to perform competitive radioligand binding assays instead of saturation binding. This was

Molecular Pharmacology Fast Forward. Published on August 28, 2012 as DOI: 10.1124/mol.112.080275
This article has not been copyedited and formatted. The final version may differ from this version.

due to the limited stock of [^{3}H]7α,25-OHC available and the large collection of mutants we generated. We confirmed that almost all of these mutants have reduced or abolished binding to [^{3}H]7α,25-OHC. For example, when Arg87 in TM2 was mutated to Ala or Trp, radioligand binding was greatly diminished (3% or 17.59% of wildtype). Consequently, in GTPγS binding assay, the ligand potency was reduced 449- or 582-fold respectively. However, when Arg87 was mutated to Lys, another amino acid with positively-charged side-chain, it didn't have any significant effect on receptor activity or ligand binding. Previously Arg87 has been reported to be important for the constitutive activity of EBI2. We did not assess the constitutive activity of EBI2 in this study. Nevertheless, our result suggests that Arg87 is important for ligand activation of EBI2. Other transmembrane region residues that showed reduced ligand binding and receptor function after Ala mutation include: Tyr112, Tyr116 of TM3; Leu197 of TM5; Tyr260, His261 and Ile264 of TM6; Val294 and M297 of TM7 (Table 2).

Asp77 in TM2 is Important for Receptor Activation*.*

The majority of mutations that negatively impacted receptor activation were found to be also important for ligand binding. Interestingly, single amino acid change of Asp77 in TM2 to Ala retained normal ligand binding (Table 2). Neither is Asp77 involved in receptor biogenesis or trafficking, as both cell-surface and total protein expressions were of similar levels to the wildtype EBI2 (Table 2). However, this mutant receptor showed no ^{35}S-GTPγS incorporation even at 1 μM 7α,25-OHC (Fig. 3E, Table 2). Such a pharmacological profile suggests that Asp77 is not involved in ligand binding, but it might

Molecular Pharmacology Fast Forward. Published on August 28, 2012 as DOI: 10.1124/mol.112.080275
This article has not been copyedited and formatted. The final version may differ from this version.

be important for receptor activation or signal transduction. An aspartic acid in TM2 is a highly conserved residue amongst family A GPCRs. In the available GPCR crystal structures, this aspartic acid sits below the ligand binding site in what is considered a water channel and is important for transmission of the signal upon ligand binding to the G-protein binding site on the intracellular side of the GPCR (Angel et al., 2009).

Homology Modeling of Human EBI2 and Ligand Docking.

The β2AR structure (PDB code 2RH1) has 52.9% sequence similarity to EBI2 in the transmembrane regions. Therefore it was used as base template for building a homology model. During manual refinement after a multiple sequence alignment with family A GPCRs (Mirzadegan et al., 2003), we found that TM2 of EBI2 shares similar structural feature to that of CXCR4 (PDB code 3ODU) because of the proline residue in this region (Pro85 in EBI2 and Pro92 in CXCR4, Fig. 4A). In addition, ECL2 of EBI2 shares higher sequence similarity to CXCR4 (35%) than to β2AR (24%) (Fig. 4B). Therefore, CXCR4 was used as the template structure for the TM2 and ECL2 regions of EBI2. For modeling of the ligand binding site, 7α,25-OHC was manually docked based on results from our structure-activity studies. The three hydroxyl groups (3'-, 7'-, and 25'- position) of 7α,25-OHC were identified to be essential for receptor-ligand interaction and were used to orient the ligand. The final model of EBI2 with 7α,25-OHC docked is shown in Fig.4C-D. As illustrated in our proposed model, Arg87 of EBI2 interacts with 7α'-hydroxyl group of 7α,25-OHC, Asn114 interacts with 25'-hydroxyl group, and Glu183 interacts with 3'-hydroxyl group. Asp77 sits just below the modeled ligand binding site and likely plays a

Molecular Pharmacology Fast Forward. Published on August 28, 2012 as DOI: 10.1124/mol.112.080275
This article has not been copyedited and formatted. The final version may differ from this version.

role in signal transmission and receptor activation. Residues Tyr112, Tyr116, Leu197, His261, Val294, and Met297 form hydrophobic interactions with the steroidal body of 7α,25-OHC.

Discussion

The Importance of the Three Hydroxyl Groups in 7α,25-OHC for Receptor Activation.

The identification of 7α,25-OHC as the endogenous ligand for EBI2 provides a pharmacological tool to activate the receptor *in vitro* and to investigate the molecular mechanisms behind EBI2 activation (Liu et al., 2011; Hannedouche et al., 2011). Here we used a mutagenesis approach to identify the residues in EBI2 critical for receptor function or ligand binding. We previously tested over 40 oxysterols and cholesterol derivatives against EBI2 and validated 7α,25-OHC as the most potent ligand. We were also able to extrapolate structure-activity correlations from these results to help elucidate the key molecular drivers involved in ligand activation. Oxysterols are oxygenated derivatives of cholesterol. While cholesterol was completely inactive at EBI2, the addition of a hydroxyl group to the steroidal ring structure (as in 7α-OHC and 7β-OHC), or to the hydrocarbon tail (as in 25-OHC or 27-OHC), was able to confer agonist activity with EC_{50} values from 100 nM to low μM (Liu et al., 2011; Hannedouche et al., 2011). Furthermore, dihydroxycholesterols with two additional hydroxyl groups as compared to cholesterol, such as 7α,25-OHC, 7β,25-OHC, 7α,27-OHC and 7β,27-OHC, were found to activate

Molecular Pharmacology Fast Forward. Published on August 28, 2012 as DOI: 10.1124/mol.112.080275
This article has not been copyedited and formatted. The final version may differ from this version.

EBI2 with much higher potency. The position of the hydroxyl group is also a critical determinant. To our knowledge, adding a hydroxyl group to the 4', 5', 6', 15', 22' or 24' position was unable to induce any agonist activity (Liu et al., 2011). It is possible that only the 7', 25' or 27' positions allow the hydroxyl groups to adopt the correct conformations for contacting key residues in the ligand binding site and forming the optimal hydrogen bond interaction. Interestingly, the rank order of the active oxysterols based on functional potency (7α,25-OHC > 7α,27-OHC > 7β,25-OHC > 7β,27-OHC > 7α-OHC > 25-OHC > 7β-OHC > 27-OHC) is in good correlation with their binding affinities. It is reasonable to postulate that, to achieve the optimal interaction between the receptor and the ligand, a hydroxyl group at the 7α' position has a more favorable conformation than the 7β' position; and a second hydroxyl group at the 25' position is more favorable than the 27' position.

The 3'-hydroxyl group is native to cholesterol and is present in all the other oxysterols we tested. Although 7α,27-OHC is the second most potent agonist for EBI2, the substitution of the 3'-hydroxyl group with a keton group abolished its ability to activate EBI2. Taken together, all three hydroxyl groups (3', 7α' and 25') in 7α,25-OHC are involved in ligand binding and receptor activation, and both the position and the orientation of the hydroxyl groups play a key role in determining agonist activity.

Molecular Pharmacology Fast Forward. Published on August 28, 2012 as DOI: 10.1124/mol.112.080275
This article has not been copyedited and formatted. The final version may differ from this version.

Glu183 in ECL2 is Held by the Classic Disulfide Bridge and Caps the Ligand Binding Site.

Certain structural features are conserved among almost all members of the GPCR superfamily, one of which is a disulfide bridge formed between a conserved Cys residue in ECL2 and another conserved Cys residue in ECL1 near the top of TM3 (Gether 2000; Karnik et al., 2003). Present in more than 90% of all GPCRs, this covalent linking is well-acknowledged to be important for the tertiary integrity of GPCRs, ligand gating and even ligand binding (Klco et al., 2005). Our data suggest Cys104 and Cys181 are functionally more equivalent while Cys21 is more similar to Cys280, supporting our hypothesis that Cys104 (ECL1) and Cys181 (ECL2) form the classic disulfide bond while Cys21 (N-terminal) and Cys280 (ECL3) may form a second disulfide bridge. This pattern of extracellular disulfide bridges is the same as in CXCR4, which also has four extracellular Cys residues distributed in the N-terminal, ECL1, ECL2 and ECL3 respectively. The crystal structure of CXCR4 confirmed the two disulfide bridges: Cyc109-Cys186 linking ECL2 with the extracellular end of TM3; and Cys28-Cys274 that connects the N-terminal to the extracellular tip of TM7 (Wu et al., 2010).

This proposed model of two disulfide bridges has important functional implications. Because of the Cys104-Cys181 link, ECL2 is brought close to the transmembrane domain and may form a cap over the putative ligand binding site (Fig. 4C), similar to what has been observed in most GPCRs. ECL2 is thus potentially positioned to interact with the ligand. Glu183, just two residues away from Cys181, is the best candidate for

Molecular Pharmacology Fast Forward. Published on August 28, 2012 as DOI: 10.1124/mol.112.080275
This article has not been copyedited and formatted. The final version may differ from this version.

forming a hydrogen bond interaction with one of the hydroxyl groups of 7α,25-OHC. Our mutagenesis data confirmed Ala substitution at Glu183 disrupted ligand binding and receptor activity (Fig.3B, Table 2), supporting our hypothesis that Glu183 is held by the disulfide bridge over the ligand binding pocket so the hydroxyl group of 7α,25-OHC can interact with the Glu183 carboxylate group. The inactivity of 7α,27-dihydroxy-4-cholesten-3-one provided more evidence that the 3'-hydroxyl interacts with Glu183, since a ketone interacting with the carboxylate would be energetically unfavorable. Taken together, the results suggest an important structural role for ECL2 in ligand activation of EBI2.

Molecular Modeling of the Ligand Binding Pocket of EBI2.

EBI2 is the first GPCR known to bind an oxysterol as endogenous ligand (Liu et al., 2011; Hannedouche et al., 2011). Therefore, it is of particular interest to understand how 7α,25-OHC interacts with EBI2 and which molecular determinants are critical for this interaction. The β2AR structure (PDB code 2RH1) has 52.9% sequence similarity to EBI2 in the transmembrane regions and was used as base template for building EBI2 homology model. However, for EBI2 TM2, CXCR4 TM2 was chosen over β2AR as a template. This is because Pro85 in EBI2 TM2 aligns with Pro92 in CXCR4 TM2, while in β2AR the proline (Pro88) is shifted by one residue (Fig. 4A). Proline residues break helical secondary structures forming a kink in the helix. Shifting a proline residue by even a single position would cause the remaining helix to kink to a slightly different orientation. Arg87, which sits two residues above Pro85, was crucial for ligand binding. Therefore,

Molecular Pharmacology Fast Forward. Published on August 28, 2012 as DOI: 10.1124/mol.112.080275
This article has not been copyedited and formatted. The final version may differ from this version.

we used CXCR4 TM2 as a template to ensure the helix would kink in the correct position and orient the remaining downstream residues, including Arg87, in a proper orientation. The crystal structures of GPCRs show very different ECL2 loop structures. ECL2 of CXCR4 was chosen as the template for EBI2 as it has similar length and the highest sequence similarity (35%) to EBI2 amongst the available GPCRs with known crystal structures (Fig. 4B). This created a hybrid structure in which β2AR was used as the base structure, while TM2 was kinked and ECL2 was modeled as in CXCR4. The use of hybrid template for GPCR homology model has been previously reported (Worth et al., 2009; Worth et al., 2011).

After building the EBI2 homology model based on the hybrid β2AR-CXCR4 template, 7α,25-OHC was manually docked into the ligand binding site. Of all the residues that were identified to be important for ligand binding, Arg87, Asn114, and Glu183 are polar or charged residues that might interact with the three hydroxyl groups in 7α,25-OHC. As expected, alanine mutations for Arg87, Asn114, and Glu183 led to functional disruption and were subsequently used to orient the ligand and optimize the EBI2 homology model (Figure 4). In the final docked model, 7α,25-OHC is oriented with 25'-hydroxyl interacting with Asn144 carboxamide group, 7α'-hydroxyl with Arg87 guanidinium group, and 3'-hydroxyl (native to cholesterol) interacting with the Glu183 carboxylate group (Fig. 4C,D). The orientation of Arg87 with the 7α'-hydroxyl group is consistent with the observation that 7α,25-OHC is more potent than 7β,25-OHC in activating EBI2. Since the steroidal body of 7α,25-OHC is rigid, a hydroxyl group in the 7β'-conformation would be

Molecular Pharmacology Fast Forward. Published on August 28, 2012 as DOI: 10.1124/mol.112.080275
This article has not been copyedited and formatted. The final version may differ from this version.

constrained and hinder the optimal contact with the guanidinium group in Arg87. Interestingly, it has been previously reported that Arg87 may act as a positive regulator for the constitutive activity of EBI2, because substitution of Arg87 by Ala, but not Lys, significantly reduced constitutive activity (Benned-Jensen and Rosenkilde, 2008). This is in line with our finding that Arg87Ala mutation, but not Arg87Lys, resulted in reduced ligand activation, suggesting that Arg87 may serve as an important molecular switch between the inactive and active states of EBI2.

The interaction between Asn114 and the 25'-hydroxyl group provides the structural basis for the better potency of 7α,25-OHC compared to 7α,27-OHC, because the hydroxyl group at the 27'-position would not reach Asn114 as close for an optimal interaction. Other supporting evidence for the putative orientation of 7α,25-OHC includes the observation that M297I mutation, but not M297A, decreased ligand binding. In the docked homology model, M297 lies tightly against the steroidal body of 7α,25-OHC. A more bulky branched chain amino acid such as Ile at this position would make unfavorable steric interaction with the rigid steroidal ring structure of the ligand.

In conclusion, our results suggest all three hydroxyl groups (3', 7α' and 25') of the ligand are important for receptor binding and activation, with 3'-hydroxyl group interacting with Glu183, 7α'-hydroxyl group interacting with Arg87, and 25'-hydroxyl group interacting with Asn114. The proposed EBI2 homology model in this report captures the critical

Molecular Pharmacology Fast Forward. Published on August 28, 2012 as DOI: 10.1124/mol.112.080275
This article has not been copyedited and formatted. The final version may differ from this version.

chemical and structural features of the binding pocket, and may be useful for future structure-based drug discovery efforts.

Molecular Pharmacology Fast Forward. Published on August 28, 2012 as DOI: 10.1124/mol.112.080275
This article has not been copyedited and formatted. The final version may differ from this version.

Authorship Contributions

Participated in research design: Zhang, Shih, Yang, Wu, Mirzadegan, Sun, Lovenberg and Liu.

Conducted experiments: Zhang, Shih, Yang, Kuei, and Liu.

Contributed new reagents or analytic tools: Wu, Deng, and Mani.

Performed data analysis: Zhang, Shih, Yang, Kuei, Mirzadegan and Liu.

Wrote or contributed to the writing of the manuscript: Zhang, Shih, Yang, Mirzadegan, Sun, Lovenberg, and Liu.

Molecular Pharmacology Fast Forward. Published on August 28, 2012 as DOI: 10.1124/mol.112.080275
This article has not been copyedited and formatted. The final version may differ from this version.

References

Angel TE, Chance MR, Palczewski K (2009) Conserved waters mediate structural and functional activation of family A (rhodopsin-like) G protein-coupled receptors. *Proc Natl Acad Sci U S A.* 106:8555-8560.

Benned-Jensen T, Smethurst C, Holst PJ, Page KR, Sauls H, Sivertsen B, Schwartz TW, Blanchard A, Jepras R, and Rosenkilde MM (2011) Ligand modulation of the Epstein-Barr virus-induced seven-transmembrane receptor EBI2: identification of a potent and efficacious inverse agonist. *J Biol Chem* 286:29292-29302.

Benned-Jensen T, Rosenkilde MM (2008) Structural motifs of importance for the constitutive activity of the orphan 7TM receptor EBI2: analysis of receptor activation in the absence of an agonist. *Mol Pharmacol*. 74:1008-1021.

Birkenbach M, Josefsen K, Yalamanchili R, Lenoir G, and Kieff E (1993) Epstein-Barr virus-induced genes: first lymphocyte-specific G protein-coupled peptide receptors. *J Virol* 67:2209-2220.

Cherezov V, Rosenbaum DM, Hanson MA, et al. (2007) High-resolution crystal structure of an engineered human beta2-adrenergic G protein-coupled receptor. Science 318: 1258-1265.

Gatto D, Paus D, Basten A, Mackay CR, and Brink R (2009) Guidance of B cells by the orphan G protein-coupled receptor EBI2 shapes humoral immune responses. *Immunity* 31:259-269.

Gatto D, Wood K, and Brink R (2011) EBI2 operates independently of but in cooperation with CXCR5 and CCR7 to direct B cell migration and organization in follicles and the germinal center. *J Immunol* 187:4621-4628.

Gether U (2000) Uncovering molecular mechanisms involved in activation of G protein-coupled receptors. *Endocr Rev* 21:90-113.

Hannedouche S, Zhang J, Yi T, Shen W, Nguyen D, Pereira JP, Guerini D, Baumgarten BU, Roggo S, Wen B, Knochenmuss R, Noël S, Gessier F, Kelly LM, Vanek M, Laurent S, Preuss I, Miault C, Christen I, Karuna R, Li W, Koo DI, Suply T, Schmedt C, Peters EC, Falchetto R, Katopodis A, Spanka C, Roy MO, Detheux M, Chen YA, Schultz PG, Cho CY, Seuwen K, Cyster JG, and Sailer AW (2011) Oxysterols direct immune cell migration via EBI2. *Nature* 475:524-527.

Karnik SS, Gogonea C, Patil S, Saad Y, Takezako T (2003) Activation of G-protein-coupled receptors: a common molecular mechanism. *Trends Endocrinol Metab* 14:431-437.

Kelly LM, Pereira JP, Yi T, Xu Y, and Cyster JG (2011) EBI2 guides serial movements of activated B cells and ligand activity is detectable in lymphoid and nonlymphoid tissues. *J Immunol* 187:3026-3032.

Klco JM, Wiegand CB, Narzinski K, Baranski TJ (2005) Essential role for the second extracellular loop in C5a receptor activation. *Nat Struct Mol Biol* 12:320-326.

Liu C, Yang XV, Wu J, Kuei C, Mani NS, Zhang L, Yu J, Sutton SW, Qin N, Banie H, Karlsson L, Sun S, and Lovenberg TW (2011) Oxysterols direct B-cell migration through EBI2. *Nature* 475:519-523.

Liu C, Eriste E, Sutton S, Chen J, Roland B, Kuei C, Farmer N, Jörnvall H, Sillard R, and Lovenberg TW (2003) Identification of relaxin-3/INSL7 as an endogenous ligand for the orphan G-protein-coupled receptor GPCR135. *J Biol Chem* 278: 50754–50764.

Liu C, Wilson SJ, Kuei C, Lovenberg TW (2001) Comparison of human, mouse, rat, and guinea pig histamine H4 receptors reveals substantial pharmacological species variation. *J Pharmacol Exp Ther* 299:121-130.

Mirzadegan T, Benko¨ G, Filipek S, and Palczewski K (2003) Sequence analyses of G-protein-coupled receptors: similarities to rhodopsin. *Biochemistry* 42:2759-2767.

Pereira JP, Kelly LM, Xu Y, and Cyster JG (2009) EBI2 mediates B cell segregation between the outer and centre follicle. *Nature* 460:1122-1126.

Pereira JP, Kelly LM, and Cyster JG (2010) Finding the right niche: B-cell migration in the early phases of T-dependent antibody responses. *Int Immunol* 22:413-419.

Rose KA, Stapleton G, Dott K, Kieny MP, Best R, Schwarz M, Russell DW, Björkhem I, Seckl J, and Lathe R (1997) Cyp7b, a novel brain cytochrome P450, catalyzes the synthesis of neurosteroids 7α-hydroxy dehydroepiandrosterone and 7α-hydroxy pregnenolone. *Proc Natl Acad Sci USA* 94:4925–4930.

Rosenkilde MM, Benned-Jensen T, Andersen H, Holst PJ, Kledal TN, Luttichau HR, Larsen JK, Christensen JP, and Schwartz TW (2006) Molecular pharmacological phenotyping of EBI2. An orphan seven-transmembrane receptor with constitutive activity. *J Biol Chem* 281: 13199-13208.

Vassilatis DK, Hohmann JG, Zeng H, Li F, Ranchalis JE, Mortrud MT, Brown A, Rodriguez SS, Weller JR, Wright AC, Bergmann JE, and Gaitanaris GA (2003) The G protein-coupled receptor repertoires of human and mouse. *Proc Natl Acad Sci* USA 100: 4903–4908.

Worth CL, Kleinau G, Krause G (2009) Comparative sequence and structural analyses of G-protein-coupled receptor crystal structures and implications for molecular models. *PLoS One* 4:e7011.

Worth CL, Kreuchwig A, Kleinau G, Krause G (2011) GPCR-SSFE: a comprehensive database of G-protein-coupled receptor template predictions and homology models. *BMC Bioinformatics*. 12:185.

Wu B, Chien EY, Mol C.D. et al. (2010) Structures of the CXCR4 chemokine GPCR with small-molecule and cyclic peptide antagonists. Science 330:1066-1071.

Molecular Pharmacology Fast Forward. Published on August 28, 2012 as DOI: 10.1124/mol.112.080275
This article has not been copyedited and formatted. The final version may differ from this version.

Footnote

Current address (X.V.Y.): Regulus Therapeutics, 3545 John Hopkins Court, San Diego, California 92121, USA

Molecular Pharmacology Fast Forward. Published on August 28, 2012 as DOI: 10.1124/mol.112.080275
This article has not been copyedited and formatted. The final version may differ from this version.

Figure Legends

Figure 1. **A,** Amino acid sequence comparison between human, rat and mouse EBI2. Underlined sequences indicate transmembrane regions. B**,** Diagram showing amino acid sequence and the predicted transmembrane regions of human EBI2. Residues shown in color (grey, green and red) are the positions where mutations were introduced. Residues in red were found to be important for receptor ligand binding or receptor activation. Residues in green, including the four Cys residues in the extracellular region, affected receptor expression when mutated to Ala. Residues shown in grey had little or no effect on the receptor pharmacology. Solid line indicates the classic disulfide bond between Cys104 and Cys181. Dashed line indicates the potential second disulfide bridge between Cys21 and Cys280.

Figure 2. Structure-Activity Studies of EBI2 **A,** Structures of Cholesterol, 7α,25-OHC, 7α,27-OHC, and 7α,27-dihydroxy-4-cholesten-3-one. **B,** Comparison of EBI2 activation by 7α,25-OHC, 7α,27-OHC and 7α,27-dihydroxy-4-cholesten-3-one in GTPγS binding assay. The assay was performed in triplicate and the values represent Mean ± SEM. The results were analyzed with GraphPad Prism 5 (GraphPad, San Diego, CA) and the EC_{50} and E_{max} values are listed in Table 1.

Figure 3. Pharmacological characterization of selected EBI2 mutants in the ^{35}S-GTPγS binding assay. Ligand-stimulated ^{35}S-GTPγS incorporations are normalized to basal ^{35}S-GTPγS incorporation in the absence of ligand and expressed as the percentage of

Molecular Pharmacology Fast Forward. Published on August 28, 2012 as DOI: 10.1124/mol.112.080275
This article has not been copyedited and formatted. The final version may differ from this version.

maximum response of the wildtype EBI2. The assay was performed in triplicate and the values represent Mean ± SEM. The results were analyzed with GraphPad Prism 5 (GraphPad, San Diego, CA). The EC_{50} values and E_{max} values are listed in Table 2. Membranes from cells expressing wildtype human EBI2 (WT) and cells that were only transfected with G_{O2} were used as a positive control and negative control (NC) respectively.

Figure 4. **A**, Sequence alignment of EBI2 transmembrane helix 2 with that of β2AR and CXCR4. CXCR4 was chosen as the template for modeling EBI2 helix 2 due to the position of the proline at position 21 versus at position 22 in β2AR. **B.** Sequence alignment of EBI2 extracellular loop 2 with that of β2AR and CXCR4. **C**, Homology model of EBI2 with 7α,25-OHC docked. The homology model was created using CXCR4 (pdb 3ODU) as a template for helix 2 and extracellular loop 2. Each of the CXCR4 segments were separately aligned to β2AR (PDB 2RH1) which was used as a template for the remaining helices and loops. 7α,25-OHC was manually docked in the EBI2 homology model using available SAR data. The hydroxyl groups of 7α,25-OHC interact with residues Arg87, Asn114, and Glu183 on EBI2. Residue Asn77 is not involved in ligand binding but is highly conserved and important for the transmission of the GPCR signal. The disulfide bond formed by Cys104 and Cys181 are structurally important in maintaining the position of the ECL2 loop which partially caps the ligand binding site as well as positioning of Glu183. **D**, Close-up view of the ligand binding site of EBI2. 7α,25-OHC is oriented in the binding site of EBI2 with the 25'-hydroxyl interacting with Asn144

Molecular Pharmacology Fast Forward. Published on August 28, 2012 as DOI: 10.1124/mol.112.080275
This article has not been copyedited and formatted. The final version may differ from this version.

carboxamide group, 7α'-hydroxyl with Arg87 guanidinium group and the 3'-hydroxyl (native to cholesterol) interacting with the E183 carboxylate group. The remaining residues Tyr112, Tyr116, Leu197, His261, Val294, and Met297 form hydrophobic interactions with the steroidal body of 7α,25-OHC.

Molecular Pharmacology Fast Forward. Published on August 28, 2012 as DOI: 10.1124/mol.112.080275
This article has not been copyedited and formatted. The final version may differ from this version.

Table 1. Effect of Ligand Structure on EBI2 Activation

Ligand	^{35}S-GTPγS Binding	
	EC_{50} (nM)	E_{max} (% of wildtype)
7α,25-OHC	0.11 ± 0.03	100
7α,27-OHC	0.97 ± 0.24	80.84 ± 4.62
7α,27-dihydroxy-4-cholesten-3-one	ND	

Comparison of the potency and efficacy of 7α,25-OHC, 7α,27-OHC, and 7α,27-dihydroxy-4-cholesten-3-one in activating EBI2 using ^{35}S-GTPγS binding assay. The EC_{50} values are concentrations of compounds that stimulated 50% of the maximal response for the wildtype EBI2. The E_{max} values are expressed as the percentage of the maximum response of the wildtype EBI2 activated by 7α,25-OHC. The assays were performed in triplicate and the values represent Mean ± SEM. ND, not determined as assay did not reach saturation.

Molecular Pharmacology Fast Forward. Published on August 28, 2012 as DOI: 10.1124/mol.112.080275
This article has not been copyedited and formatted. The final version may differ from this version.

Table 2. Characterization of Selected EBI2 Mutations

Region of Residue Changed	Mutation	Receptor Expression		^{35}S-GTPγS Binding		Radioligand Binding
		Surface (% of WT)	Total (% of WT)	EC_{50} (nM)	E_{max} (% of WT)	Specific Binding (% of WT)
	WT-EBI2	100.00	100.00	0.11 ± 0.03	100	100.00
N-terminal	C21A	20.68	59.97	2.29 ± 0.82	23.36 ± 1.21	5.42 ± 3.39
ECL1	C104A	2.75	90.22	NA		NA
ECL2	C181A	5.49	79.51	NA		NA
	E183A	59.82	74.26	5.46 ± 2.00	53.90 ± 2.07	11.33 ± 1.47
ECL3	C280A	32.60	53.24	0.93 ± 0.07	50.26 ± 2.00	16.56 ± 3.29
TM2	P85A	17.44	62.42	2.16 ± 1.67	27.28 ± 8.37	6.37 ± 1.43
	Y90A	23.56	80.78	23.74 ± 3.25	39.74 ± 1.81	NA
	D77A	86.97	78.50	NA		99.31 ± 5.86
	R87A	110.84	117.04	49.04 ± 7.72	49.97 ± 1.01	NA
	R87W	77.13	144.55	64.01 ± 4.01	76.17 ± 0.86	17.59 ± 8.72
	R87K	75.63	78.64	3.99 ± 0.36	78.21 ± 1.43	78.02 ± 9.35
TM3	N114A	47.63	77.51	NA		15.98 ± 5.04
	Y112A	91.83	89.34	11.42 ± 2.49	96.01 ± 3.22	9.39± 4.04
	Y116A	118.08	110.49	9.13 ± 0.92	51.71 ± 4.99	NA
TM5	L197A	105.57	116.52	11.78 ± 0.76	87.93 ± 3.36	20.21± 1.77
TM6	F257A	35.86	45.06	0.11 ± 0.21	36.74 ± 3.43	15.85 ± 2.26
	Y260A	114.07	125.93	140.50 ± 6.87	125.90 ± 2.15	NA
	H261A	79.95	97.96	63.71 ± 17.19	44.81 ± 3.68	4.65 ± 1.54
	I264A	112.03	104.26	1.72 ± 0.49	73.30 ± 7.87	10.84 ± 3.48
TM7	V294A	74.29	137.79	3.11 ± 4.60	80.37 ± 4.42	47.65 ± 2.24
	M297I	105.34	90.98	4.09 ± 0.42	92.88 ± 2.09	36.95 ± 3.71
	M297A	110.75	142.23	0.68 ± 0.04	158.5 ± 4.63	93.55 ± 5.05

Molecular Pharmacology Fast Forward. Published on August 28, 2012 as DOI: 10.1124/mol.112.080275
This article has not been copyedited and formatted. The final version may differ from this version.

Recombinant EBI2 mutant receptors were characterized by receptor expression analysis, ^{35}S-GTPγS assay and radioligand binding assay.

Total and cell-surface expression was detected by anti-V5-antibody in ELISA assay either in the presence or absence of 1% Triton-X-100 as the penetration reagents. The expression of N-terminal tagged V5-EBI2 is expressed as 100%. Cells without recombinant protein expression or with C-terminally V5-tagged GPR81 (GPR81-V5) were used as negative controls for protein expression.

For the ^{35}S-GTPγS binding assay, the EC_{50} values are 7α,25-OHC concentrations that stimulated 50% of the maximal response for each individual mutant. The E_{max} values are expressed as percentage of the maximum response of the wildtype EBI2. The assays were performed in triplicate and the values represent as Mean ± SEM. NA, no receptor stimulation by 7α,25-OHC was observed.

For the radioligand binding assay, the total specific binding for each mutant was calculated as percentage of the maximum specific [^{3}H]7α,25-OHC binding to the wildtype EBI2. NA, no specific binding was observed.

Molecular Pharmacology Fast Forward. Published on August 28, 2012 as DOI: 10.1124/mol.112.080275
This article has not been copyedited and formatted. The final version may differ from this version.

Figure 1

A

```
Human:     MANNFTPPSATPQGNDCDLYAHHSTARIVMPLHYSLVFIIGLVGNLLALVVIVQNRKKIN  64
  Rat:     MANNFTTPLAASHGNNCDLYAHHSTARILMPLHYSLVFIIGLVGNLLALVVIVQNRKKIN  60
Mouse:     MANNFTTPLATSHGNNCDLYAHHSTARVLMPLHYSLVFIIGLVGNLLALVVIVQNRKKIN  60
Consensus: MANNFT-P-A---GN+CDLYAHHSTARI+MPLHYSLVFIIGLVGNLLALVVIVQNRKKIN
                                                  TM1
Human:     STTLYSTNLVISDILFTTALPTRIAYYAMGFDWRIGDALCRITALVFYINTYAGVNFMTC  124
  Rat:     STTLYSMNLVISDILFTTALPTRIVYYALGFDWRIGDALCRITALLFYINTYAGVNFMTC  120
Mouse:     STTLYSMNLVISDILFTTALPTRIAYYALGFDWRIGDALCRVTALVFYINTYAGVNFMTC  120
Consensus: STTLYS-NLVISDILFTTALPTRI-YYA+GFDWRIGDALCRITAL+FYINTYAGVNFMTC
                      TM2                                   TM3
Human:     LSIDRFIAVVHPLRYNKIKRIEHAKGVCIFVWILVFAQTLPLLINPMSKQEAERITCMEY  184
  Rat:     LSIDRFFAVVHPLRYNKIKRIEYAKGICVFVWILVFAQTLPLLLKPMSKQEADKTTCMEY  180
Mouse:     LSIDRFFAVVHPLRYNKIKRIEYAKGVCLSVWILVFAQTLPLLLTPMSKEEGDKTTCMEY  180
Consensus: LSIDRF-AVVHPLRYNKIKRIE+AKG+C+FVWILVFAQTLPLL+-PMSKQEA++-TCMEY
                                    TM4
Human:     PNFEETKSLPWILLGACFIGYVLPLIIILICYSQICCKLFRTAKQNPLTEKSGVNKKALN  244
  Rat:     PNFEGTASLPWILLGACLLGYVLPLAIILLCYSQICCKLFRTAKQNPLTEKSGVNKKALN  240
Mouse:     PNFEGTASLPWILLGACLLGYVLPITVILLCYSQICCKLFRTAKQNPLTEKSGVNKKALN  240
Consensus: PNFE-T-SLPWILLGAC-+GYVLPL-IIL+CYSQICCKLFRTAKQNPLTEKSGVNKKALN
                         TM5
Human:     TIILIIVVFVLCFTPYHVAIIQHMIKKLRFSNFLECSQRHSFQISLHFTVCLMNFNCCMD  304
  Rat:     TIILIIGVFVLCFTPYHVAIMQHMVKTLYAPGALGCGVRHSFQISLHFTVCLMNFNCCMD  300
Mouse:     TIILIIVVFILCFTPYHVAIIQHMIKMLCSPGALECGARHSFQISLHFTVCLMNFNCCMD  300
Consensus: TIILII-VFVLCFTPYHVAI+QHM+K-L-----L-C--RHSFQISLHFTVCLMNFNCCMD
                TM6                                     TM7
Human:     PFIYFFACKGYKRKVMRMLKRQVSVSISSAVKSAPEENSREMTETQMMIHSKSSNGK     361
  Rat:     PFIYFFACKGYKRKVMKMLKRQVSVSISSAVRSAPEENSREMTESQMMIHSKASNGR     357
Mouse:     PFIYFFACKGYKRKVMKMLKRQVSVSISSAVRSAPEENSREMTESQMMIHSKASNGR     357
Consensus: PFIYFFACKGYKRKVM+MLKRQVSVSISSAV+SAPEENSREMTE+QMMIHSK+SNG+     357
```

B

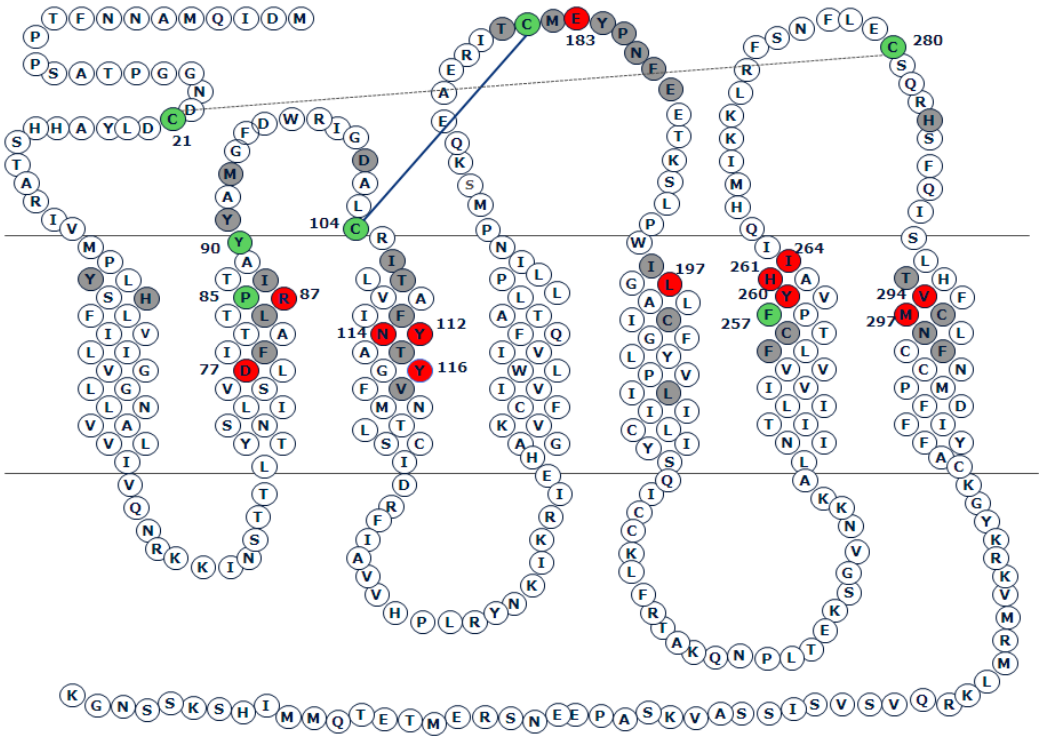

Molecular Pharmacology Fast Forward. Published on August 28, 2012 as DOI: 10.1124/mol.112.080275
This article has not been copyedited and formatted. The final version may differ from this version.

Figure 2

A

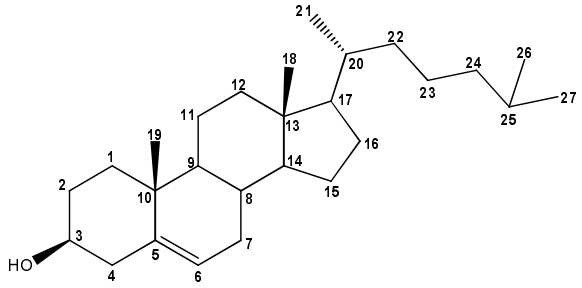

Cholesterol

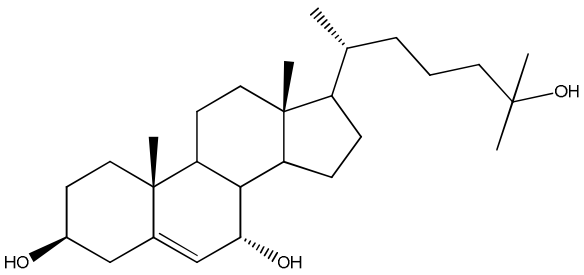

7α, 25-dihydroxycholesterol

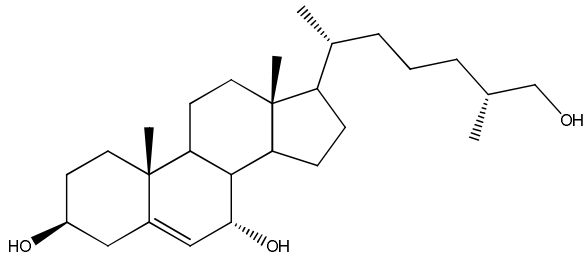

7α, 27-dihydroxycholesterol

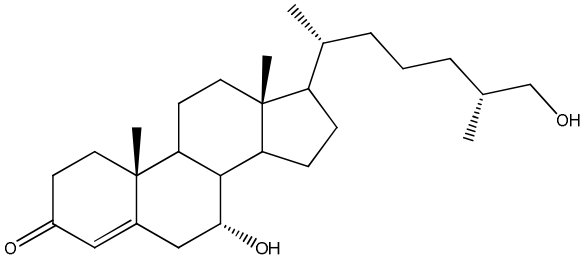

7α, 27-dihydroxy-4-cholesten-3-one

B

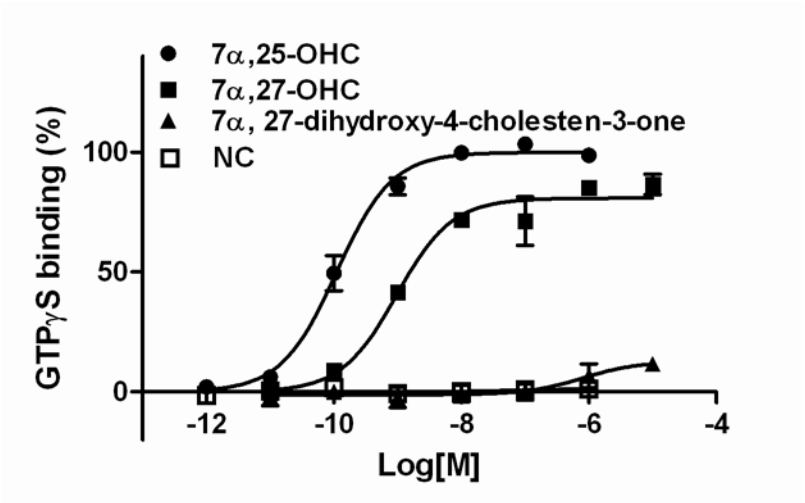

Molecular Pharmacology Fast Forward. Published on August 28, 2012 as DOI: 10.1124/mol.112.080275
This article has not been copyedited and formatted. The final version may differ from this version.

Figure 3

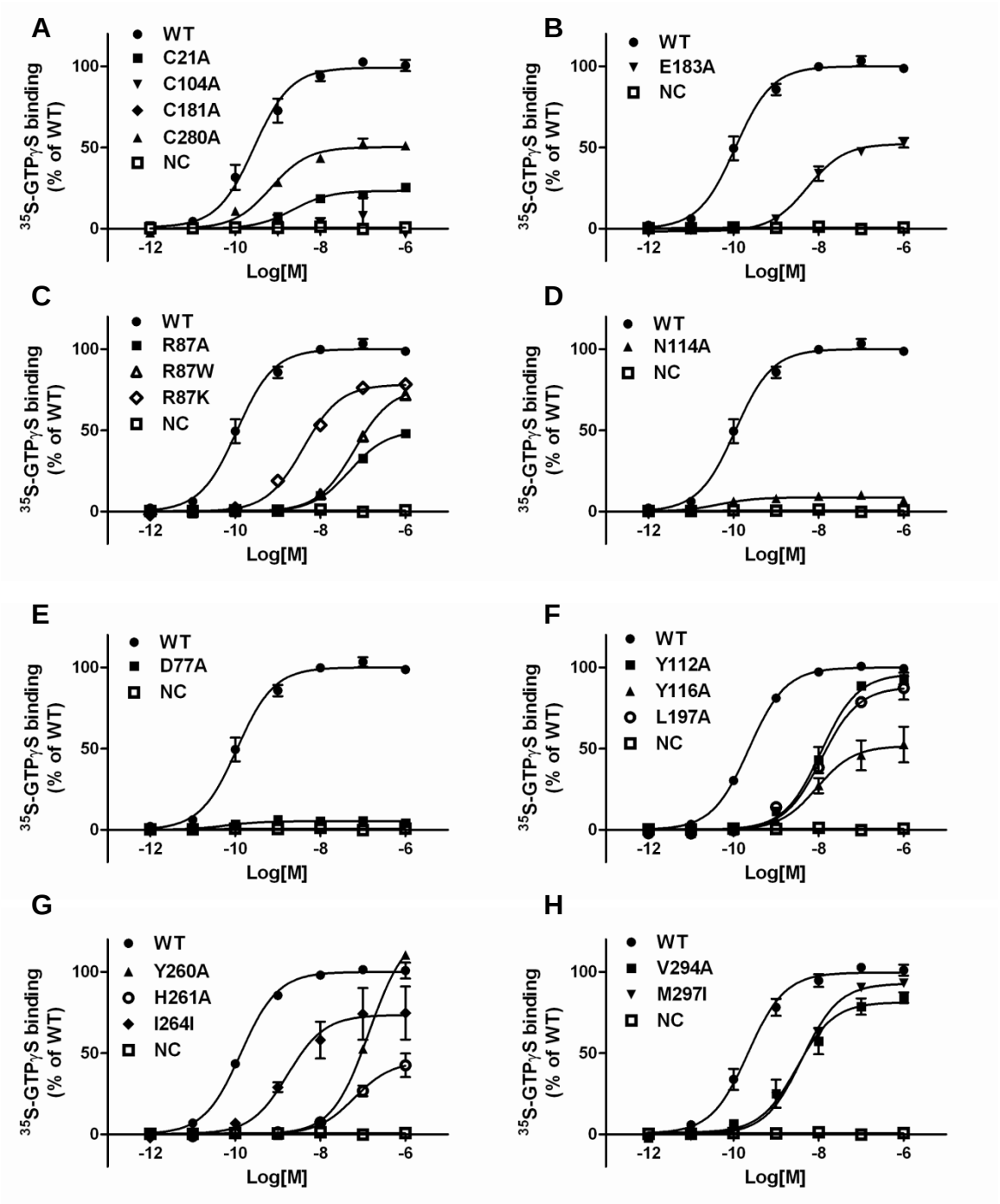

Molecular Pharmacology Fast Forward. Published on August 28, 2012 as DOI: 10.1124/mol.112.080275
This article has not been copyedited and formatted. The final version may differ from this version.

Figure 4

A

```
ADRB2_HUMAN     VTNYFITSLACADLVMGLAVVPFGAAH
CXCR4_HUMAN     MTDKYRLHLSVADLLFVITLPFWAVDA
EBI2_HUMAN      STTLYSTNLVISDILFTTALPTRIAYY
```

B

```
ADRB2_HUMAN     MHWYRATHQEAINCYANETCCDFFT
CXCR4_HUMAN     -FANVSEADDRYICDRFYPNDLWLP
EBI2_HUMAN      -NPMSKQEAERITCMEYPNFEETKS
```

C

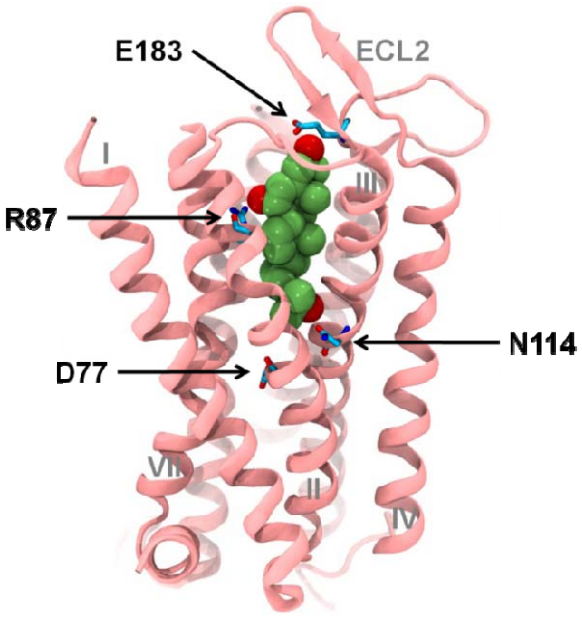

D

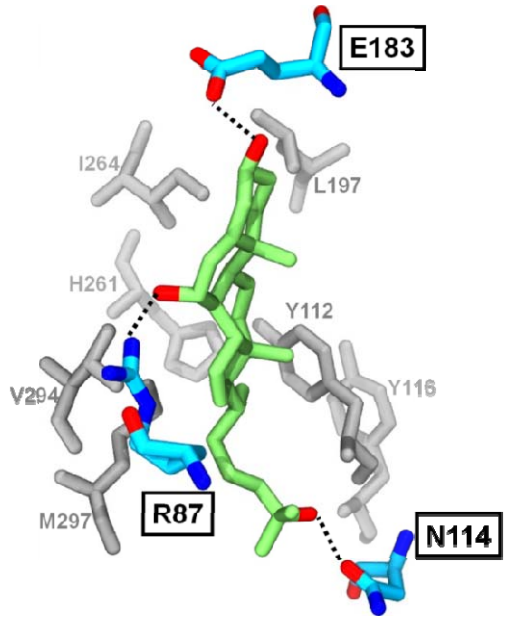

Supplemental Data

Identification of Structural Motifs Critical for EBI2 Function and Homology Modeling of Ligand Docking Site

Li Zhang, Amy Y. Shih, Xia V. Yang, Chester Kuei, Jiejun Wu, Xiaohu Deng, Neelakandha S. Mani, Tara Mirzadegan, Siquan Sun, Timothy W. Lovenberg, Changlu Liu

Supplemental Table 1. Effects of Mutations on EBI2 Function.

Region of Residue Changed	Mutation	Expression		GTPγS Binding		Radioligand Binding
		surface (% of WT)	total (% of WT)	pEC_{50}	E_{max} (% of WT)	% of WT
	WT	100.00	100.00	9.96 ± 0.07	100	100.00
N-terminal	**C21A**	20.68	59.97	8.64 ± 0.12	23.36 ± 1.21	5.42 ± 3.39
ECL1	**Y91A**	79.01	106.28	9.77 ± 0.08	47.39 ± 1.60	66.66 ± 3.82
	M93I	82.32	79.57	9.89 ± 0.16	112.6 ± 8.36	93.72 ± 5.54
	D101A	100.39	92.92	9.28 ± 0.05	154 ± 3.19	89.58 ± 2.14
	C104A	2.75	90.22	NA		NA
ECL2	**T180A**	71.76	114.21	9.98 ± 0.08	68.04 ± 2.64	55.18 ± 5.46
	C181A	5.49	79.51	NA		NA
	M182A	62.97	138.06	8.96 ± 0.11	74.30 ± 3.61	51.40 ± 2.88
	E183A	59.82	74.26	8.26 ± 0.08	53.90 ± 2.07	11.33 ± 1.47
	Y184A	79.31	130.72	9.31 ± 0.07	94.54 ± 2.76	64.74 ± 8.49
	P185A	78.63	144.95	9.72 ± 0.14	58.05 ± 3.67	55.32 ± 9.07
	N186A	99.29	116.13	9.30 ± 0.08	165.3 ± 5.46	92.23 ± 4.26
	F187A	79.67	91.21	8.84 ± 0.07	137.7 ± 4.12	30.58 ± 3.87
	E188A	127.04	99.85	9.59 ± 0.05	117.7 ± 2.71	138.60 ± 5.41
ECL3	**C280A**	32.60	53.24	9.16 ± 0.09	50.26 ± 2.00	16.56 ± 3.29
	H284Y	97.44	55.40	9.74 ± 0.11	119.9 ± 5.97	123.18 ± 3.37
TM1	**H37A**	113.69	126.17	9.37 ± 0.07	106.1 ± 3.19	166.97 ± 5.22
	Y38A	89.18	117.49	9.41 ± 0.06	80.72 ± 2.15	44.52 ± 1.96
TM2	**D77A**	86.97	78.50	NA		99.31 ± 5.86
	F80A	85.62	138.02	9.85 ± 0.11	90.5 ± 4.60	93.89 ± 10.49
	L84A	64.74	92.18	8.98 ± 0.07	104.7 ± 3.25	41.08 ± 2.68
	P85A	17.44	62.42	8.66 ± 0.22	27.28 ± 8.37	6.37 ± 1.43
	R87A	110.84	117.04	7.31 ± 0.04	49.97 ± 1.01	NA
	R87K	75.63	78.64	8.40 ± 0.04	78.21 ± 1.43	78.02 ± 9.35
	R87W	77.13	144.55	7.19 ± 0.02	76.17 ± 0.86	17.59 ± 8.72
	I88A	94.36	79.30	9.62 ± 0.10	100.2 ± 4.04	60.64 ± 3.68
	Y90A	23.56	80.78	7.62 ± 0.10	39.74 ± 1.81	NA
TM3	**I106E**	152.24	122.75	9.71 ± 0.20	98.79 ± 8.67	87.54 ± 4.30
	T107A	106.95	108.01	9.85 ± 0.03	99.12 ± 1.49	68.50 ± 3.09
	F111A	80.10	119.00	9.70 ± 0.08	102.6 ± 3.38	70.67 ± 6.17
	Y112A	91.83	89.34	7.94 ± 0.07	96.01 ± 3.22	9.39 ± 4.04
	N114A	47.63	77.51	NA		15.98 ± 5.04
	T115A	118.78	111.62	9.94 ± 0.05	97.95 ± 2.16	89.14 ± 4.17
	Y116A	118.08	110.49	8.04 ± 0.21	51.71 ± 4.99	NA
	V119A	84.07	134.29	8.83 ± 0.05	88.94 ± 1.96	33.92 ± 1.76

TM5	**I196A**	141.81	82.01	9.85 ± 0.10	129.7 ± 6.10	93.16 ± 7.38
	L197A	105.57	116.52	7.93 ± 0.08	87.93 ± 3.36	20.21 ± 1.77
	C201A	107.43	106.43	8.58 ± 0.05	74.02 ± 1.62	94.01 ± 3.95
	L209A	102.31	95.45	9.47 ± 0.10	81.58 ± 3.25	67.22 ± 2.52
TM6	**F253A**	126.80	90.08	9.58 ± 0.03	157.4 ± 2.20	58.90 ± 3.54
	C256A	98.47	102.95	9.91 ± 0.22	67.67 ± 6.75	50.26 ± 2.44
	C256F	95.16	104.10	9.67 ± 0.05	99.48 ± 2.36	81.96 ± 6.96
	F257A	35.86	45.06	9.96 ± 0.20	36.74 ± 3.43	15.85 ± 2.26
	Y260A	114.07	125.93	6.85 ± 0.03	125.9 ± 2.15	NA
	H261A	79.95	97.96	7.20 ± 0.15	44.81 ± 3.68	4.65 ± 1.54
	I264A	112.03	104.26	8.77 ± 0.25	73.3 ± 7.87	10.84 ± 3.48
TM7	**T293A**	72.31	93.74	9.43 ± 0.06	131.9 ± 3.15	82.20 ± 5.93
	V294A	74.29	137.79	8.51 ± 0.13	80.37 ± 4.42	47.65 ± 2.24
	C295A	138.60	140.52	9.37 ± 0.05	133.6 ± 2.78	127.33 ± 5.71
	M297A	110.75	142.23	9.17 ± 0.07	158.5 ± 4.63	93.55 ± 5.05
	M297I	105.34	90.98	8.39 ± 0.05	92.88 ± 2.09	36.95 ± 3.71
	N298A	104.69	88.84	9.93 ± 0.04	63.84 ± 1.11	113.89 ± 6.21
	F299A	102.55	146.20	9.22 ± 0.08	120.7 ± 2.77	100.60 ± 8.25

Recombinant EBI2 mutant receptors were characterized by receptor expression analysis, ^{35}S-GTPγS binding assay and radioligand binding assay. Total and cell surface expressions were detected with anti-V5-antibody either in the presence or absence of 1% Triton-X-100 as the permeabilization reagent. The expression of N-terminal tagged V5-EBI2 is expressed as 100%.

For ^{35}S-GTPγS binding assay, the EC_{50} values are the concentrations of 7α,25-OHC that stimulated 50% of the maximum response for each individual mutant (E_{max}). The maximum ^{35}S-GTPγS incorporation by wildtype EBI2 is set as 100%, and the E_{max} of each mutant is expressed as percentage of the maximum response of the wildtype EBI2. The assays were performed in triplicate and the values represent Mean ± SEM. NA, no receptor stimulation by 7α,25-OHC was observed.

For radioligand binding assay, the total specific binding for each mutant is calculated as percentage of the maximum specific [^{3}H]7α,25-OHC binding to the wildtype EBI2. NA, no specific binding was observed.